

THE THERMAL ANALYSIS OF A NdFeB LOUDSPEAKER MOTOR USING FINITE ELEMENT ANALYSIS.

Mark Dodd, Celestion Int. Ltd.

1. INTRODUCTION

Past papers on loudspeaker thermal behaviour have all been based on lumped element models of the motor structure.[1][2] The work described in this paper uses a simple form of the Finite Element method to explore heat in a new loudspeaker topology. This method has the advantage that few geometric approximations are required and for those skilled in the art of FEM, the time to set up a problem is minimised.

THERMAL FINITE ELEMENT METHOD

The FEM software used in this paper was developed for applications such as electric motors and induction heating, although it does not model fluid flow it does offer the capability of coupling thermal, magnetic and electrical problems [4]. For the sake of simplicity this paper looks only at the thermal domain.

Static Thermal FEM

The static FEM used in this paper is based on equation 1 where Q_H is the thermal source density or dissipated power [4] and T is the temperature. Static FEM solves for the settled temperature when the system has reached thermal equilibria and the only material property required is thermal conductivity.

$$\nabla \cdot (-k\nabla(T)) = Q_H \quad [1]$$

Heat loss from the model is achieved by means of the non-homogenous Neuman boundary condition:

$$k \frac{dT}{dn} = -F_H - h(T - T_a) - \xi\sigma(T^4 - T_a^4) \quad [2]$$

Where T_a is the ambient temperature, dn is an incremental distance along the boundary, F_H is thermal flux from outside, and h is the heat transfer coefficient for convection.

Transient Thermal FEM

The transient analysis is based on the equations 3 and 4 which both include the specific heat capacity and dT/dt the rate of change of temperature with time. For this analysis both the specific heat capacity and thermal conductivity are required. The solution is solved in timesteps small enough to allow only a small change of temperatures between steps.

$$\rho_c \frac{dT}{dt} + \nabla \cdot (-k\nabla(T)) = Q_H \quad [3]$$

The non homogenous Neuman boundary condition for the transient case is given below:

$$\rho_c \frac{dT}{dt} + k \frac{dT}{dn} = -F_H - h(T - T_a) - \xi\sigma(T^4 - T_a^4) \quad [4]$$

Application of the thermal finite element method.

A significant limitation of both the simple FEM used and lumped element analyses is that fluid flow is not predicted and empirical data is required to determine the magnitudes at forced and natural convection [1][2]. In the case of FEM, the effects of thermal conductivity and capacity may be evaluated for the desired axisymmetric or three dimensional geometry without the assumptions required to 'lump' regions into a few single dimensional elements. For this paper it was decided to use an axisymmetric geometry allowing a rapid model set-up and solution time. Due to the small size of the voice coil structure a separate model is used to develop a composite material representing both conductor and insulator of the voice coil.

Derivation of composite voice coil material properties.

As with most FEM, in Thermal FEM using more elements will give better spatial resolution and convergence towards the correct solution. The mesh should be finest in regions of rapid change of temperature, however a finer mesh will be slower to solve, the solution time being approximately proportional to the square of the number of elements. In Magnetic FEM it is possible to mesh the voice coil region with elements larger than the wire size since the voice coil region is given constant current and has constant magnetic permeability. However, in the case of thermal FEM, the heat flow within the coil depends on the dimensions and material properties of wire insulation and bonding materials. Modeling the full coil geometry would be very time-consuming and would lead to a huge number of elements so we have chosen to derive bulk thermal properties of the voice coil using an additional FEM model of the voice coil's real geometry.

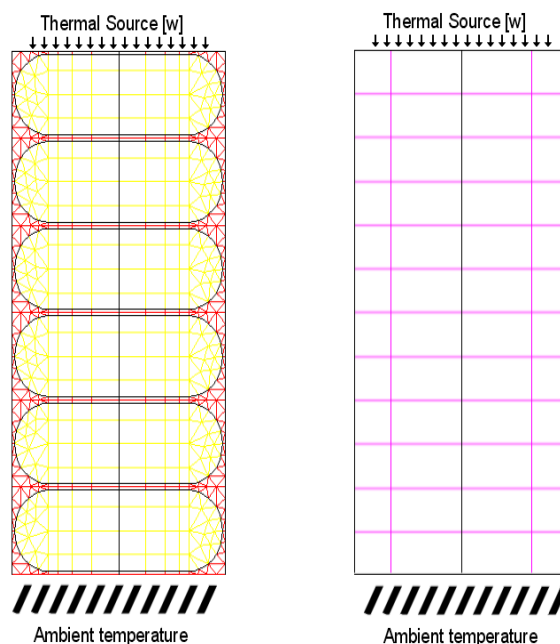


Figure 1. Full voice coil model.

The left hand region in figure 1 shows the full coil modeled with copper and insulating material. The problem is then solved for a range of values of thermal conductivity applied to the right hand mesh. The temperature adjacent to the heat source was plotted as a function of conductivity allowing the correct value of 'composite' coil conductivity to be read of the graph. The correct composite material property may be found at the intersection of the temperature curves as shown in Figure 2. Please note that the units used for temperature in the graphs throughout the paper are degrees Celsius.

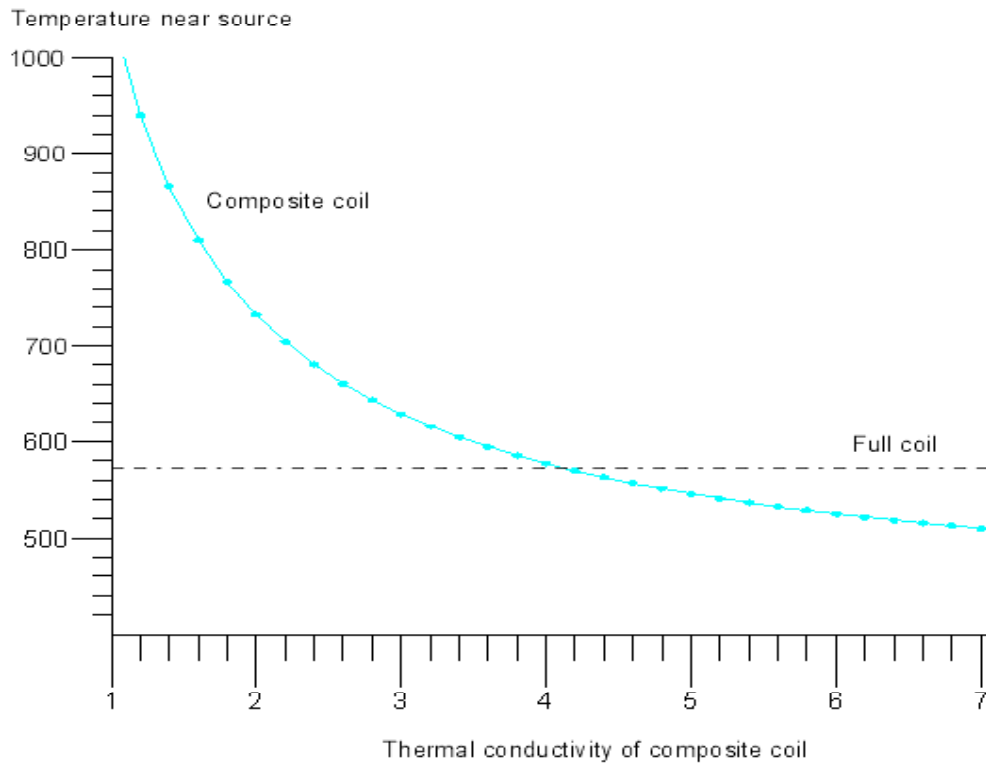


Figure 2.

Temperature of composite versus full coil FEM models.

Axisymmetric Geometry development.

Unlike the axisymmetric magnet and coil, the frame is axi-periodic, having a similar geometry to a wagon wheel. We need to create an axisymmetric geometry thermally equivalent to the 3D geometry [see figure3]. A number of factors must be considered; firstly the length and cross-sectional area of heat paths must be maintained to give the correct thermal resistance. Secondly the volume must be correct to give the correct thermal capacity. Thirdly the emissivity and convection exchange coefficients must be adjusted to give the correct heat transfer. The axisymmetric version of the frame has too much surface area and the convection and emissivity coefficients must be reduced by the ratio of actual area to modeled area.

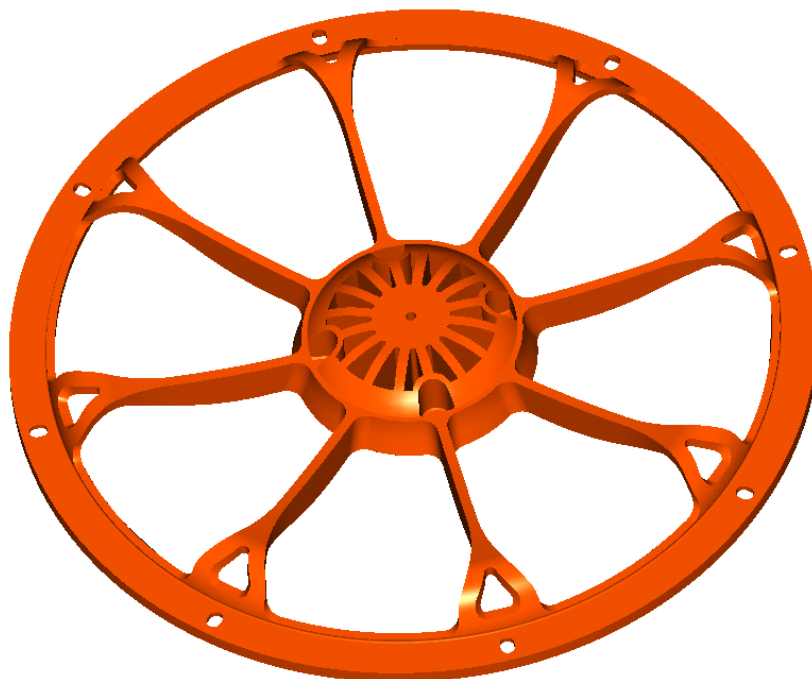


Figure 3. Nti 15 Frame

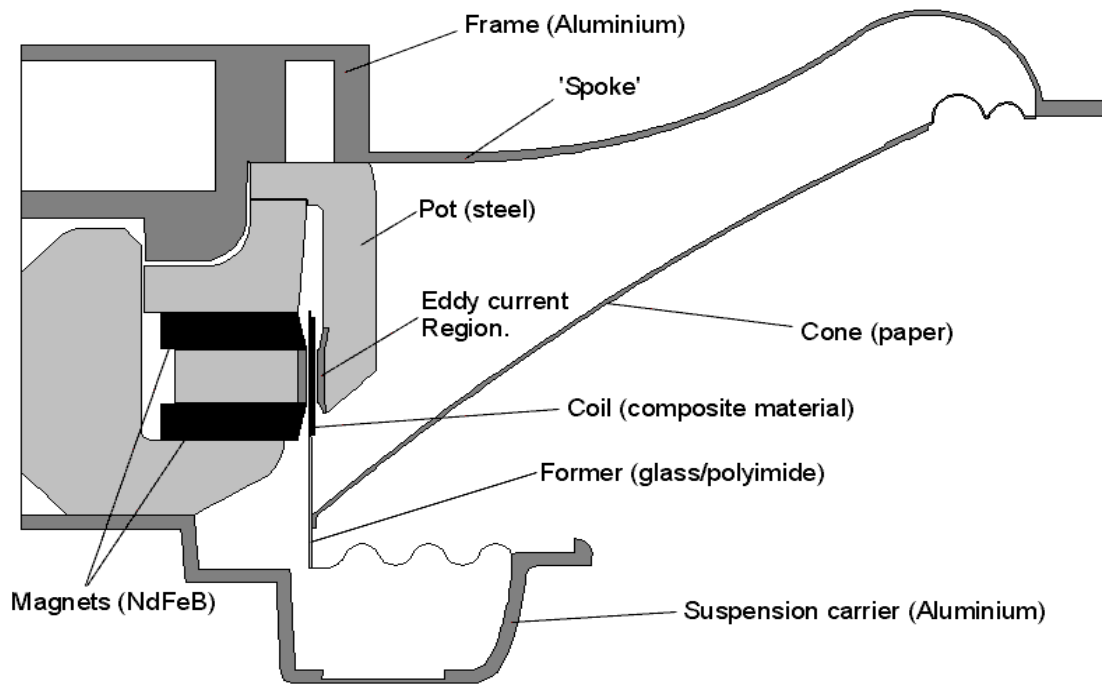


Figure 4. Axisymmetric geometry of Nti15.

The glue joints are very thin and require the use of quadrilateral elements to produce an efficient mesh. The small heat flow along the glue joint allows a large element aspect ratio avoiding the need for a very fine mesh. The complete mesh with an inset showing the mesh at one glue joint is shown in figure 5.

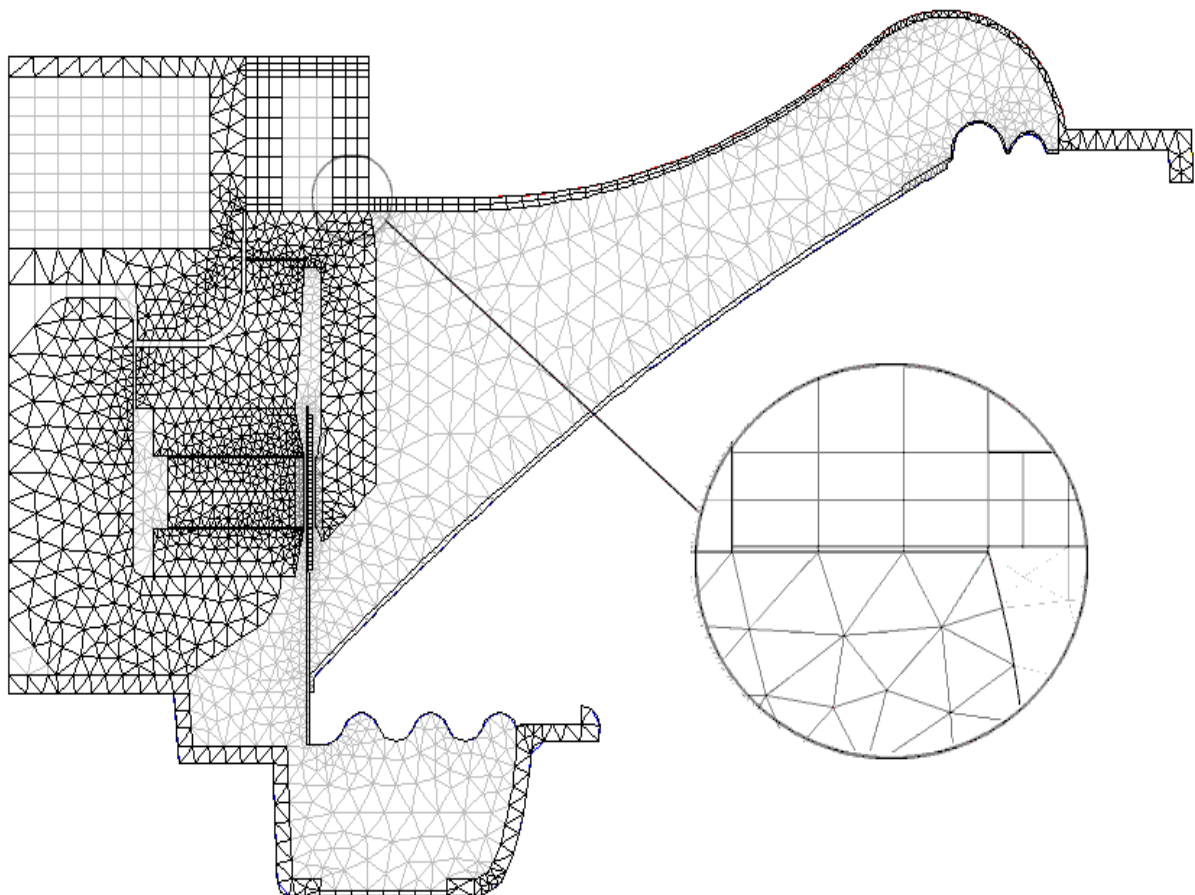


Figure 5. Picture of general mesh with glue joint detail.

Boundary Conditions

The thermal power dissipated in the coil within the model was calculated using AkaBak from electrical impedance curves measured at the appropriate power and temperature. The voice coil was modeled by a heat source with constant power density and the composite properties derived from the full voice coil model. The model also included the heating effects of eddy currents within the poles adjacent to the coil. The magnitude of the eddy currents was derived from Transient Magnetic FEM models [5] and was about 6% for the drivers without rings and 14% for the driver with Aluminium rings.

Since the thermal properties of the air are modified by air motion and the software lacks the capability to model radiation between surfaces, an effective thermal conductivity of air in the gap was derived, by inspection, from experimental results and a series of FEM solutions over ranges of values of the unknown variables. Similarly the external emissivity and convection coefficients were derived experimentally.

To evaluate the external emissivity the driver was suspended on thermally insulating mounts in a vacuum chamber with a highly absorptive interior coating. The vacuum completely eliminates any heat losses due to convection and conduction, leaving the loss due to radiation. A known power was applied to the loudspeaker, and the magnet temperature was measured when the driver reached thermal equilibrium. A FEM model of the driver in these conditions was then created using a Non Homogenous Neuman boundary in [equation 2] to model external Radiated heat loss. In the region of the spokes a correction factor was applied to the emissivity to take into account the actual area of the frame compared to the axisymmetric geometry modelled. This FEM model was solved for a range of emissivities yielding, after some iteration, a value for emissivity.

To find the convective coefficients it was necessary to measure the coil magnet and frame temperatures for the driver in free air. This allowed the convection coefficients for the air in the gap to be determined via comparison with FEM results using the radiation coefficient from the vacuum chamber experiment.

Full model and experimental results.

The first driver we will consider is the PA15, an experimental fifteen inch driver with a high efficiency NdFeB magnet and a four inch nominal diameter voice coil. The PA15 has a cast aluminium four spoke frame with a rear suspension carrier of thin pressed steel. To keep convection to a minimum it was decided to use a pink noise test signal bandpass filtered at 108Hz and 410Hz using 24dB/octave Butterworth filters at a nominal power level of 100w. The mean voice coil temperature measurement was achieved by measuring coil resistance as described in [1]. Temperature distributions are shown in table 1 for both FEM results and experimental results. The FEM temperature distributions are in good agreement with the experimental results. However, the voice coil and magnet temperatures are unacceptably high considering the desired power rating of the driver.

In an attempt to reduce the coil temperature Aluminium 'heat rings' were introduced to the ID of the coil creating the driver PA15 Alring. This reduced the thermal resistance between voice coil and magnet assembly, thereby cooling the voice coil, but also resulted in an increased magnet temperature, which is not acceptable given the thermal limitations of NdFeB. The initial results from this driver were somewhat anomalous due to the change in airflow in the gap and also a poor glue joint between frame and magnet. The results for the adjusted model are shown in table 1. Reducing the glue gap to the usual thickness gave a lower, but still unacceptable magnet temperature, leading to the abandonment of the 'heat rings' for this driver.

What transpires from the PA15 result is that the thermal resistance from the magnet assembly to ambient was too high. In order to reduce this thermal resistance, the design of the frame was re-evaluated and the number of spokes, which allow heat transfer out of the central magnet assembly region was increased. Also the suspension carrier was

Color Shade Results
Quantity : Temperature degrees C.

K(SPOKE_1) (W/m2/degree) : 20
Scale / Color

20	/	32
32	/	44
44	/	56
56	/	68
68	/	80
80	/	92
92	/	104
104	/	116
116	/	128
128	/	140
140	/	152
152	/	164
164	/	176
176	/	188
188	/	200
200	/	212

In order to evaluate the validity of this model at higher powers the experiments were repeated at 200W nominal power input. The results in table 1 again show good agreement between the FEM and measured data.

Nominal Power Frequency range of noise input. Data origin	PA15 100W 110Hz-400H		PA15 Alring 100W 110Hz-400H		Nti 15 100W 110Hz-400Hz		Nti 15 200W 110Hz-400Hz		Nti 15 100w 50Hz-400Hz	
	Meas'/ FEM		Meas/ FEM*		Meas'/ FEM		Meas'/ FEM**		Meas'/ FEM***	
T(v/c)	123	124.7	113	119	115	113	206	201	98	97
T(mag)	73.4	72.5	97	95.3	62.0	60.4	98.1	96	51.5	53.7
T(frame)	63.2	60.2	68.7	68	50.5	48.8	73.1	73.9	41.4	43.9
T(front)	60.4	60.8	67.2	69.1	50.8	49.9	71.5	75.6	42.0	4.4
T(arm)	47.4	46.4	55	52	40.4	40.3	56.9	58.2	32.4	36.7
T(rim @ arm)	31.4	30.8	31.5	33.3	26.4	30	33.0	38.1	21.7	28
T(back mid)	63.4	58.8	95	93.6	47.2	46.8			40.8	42
T(back edge)	29.8	34.5	31	27	35.7	34.3			33.2	31.9

* Frame glue joint thickness increased, air conductivity increased.

** Power input reduced by 3.6% to allow for convection form coil to ambient.

*** Power input reduced by 8% to allow for convection form coil to ambient.

Table 1

To investigate the effect of the forced convection produced by movement of the cone and coil the, NTI-15 was re-measured with a 50Hz rather than 108Hz cut off. This produced an 8% temperature decrease in the coil temperature. To model this thermal short circuit, a reduction in input power was applied such that the magnitude of the temperature distributions agreed with experiment. Once again the problem was solved over a range of parameter values to find the correct input power so the temperature distribution could be checked. It was somewhat gratifying to find that this approach gave good agreement with the measured results.

TRANSIENT SOLUTION

Having set up the model it may then be solved as transient problem, in our case for a constant heat input. The results of a transient solution For the Nti 15 driver are illustrated in Figure 7 and figure 8. These show how the temperature distribution along the coil develops with time and how the temperature rises at various points in the driver respectively. It can be seen that the time-constant gets larger for points further from the voice coil.

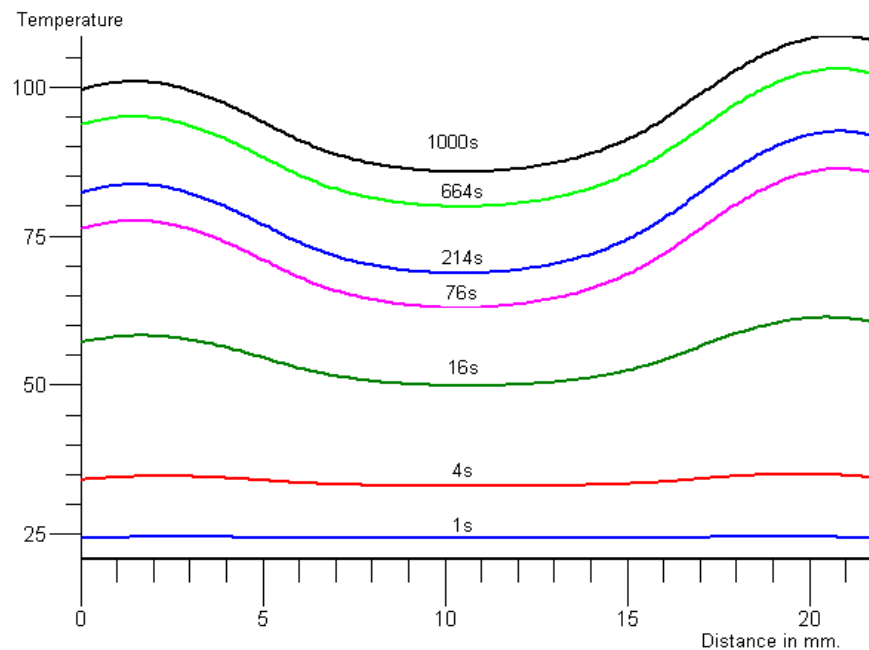


Figure 7. Temperature through the coil plotted at various times.

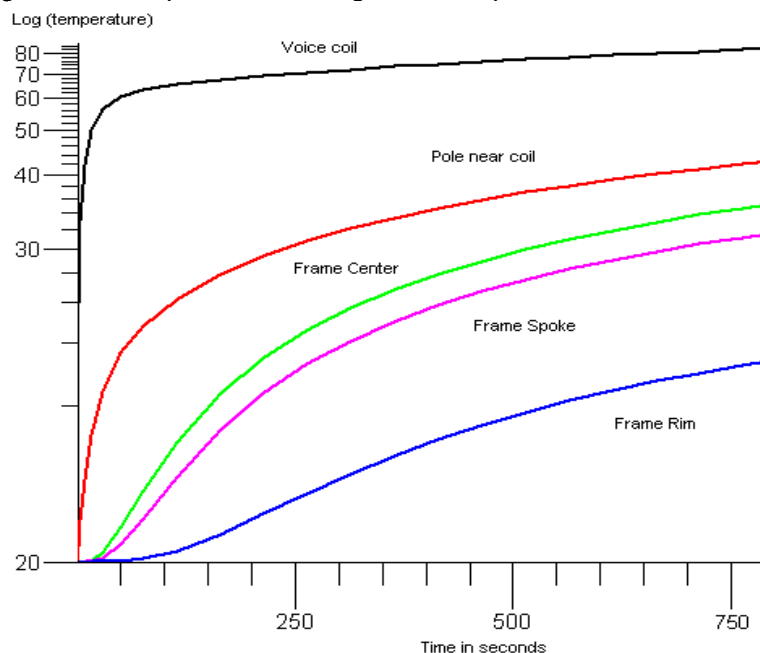


Figure 8. Temperature of various points throughout the driver plotted as a function of time.

CONCLUSION

Thermal FEM can provide a method of quickly and inexpensively experimenting with design parameters. Experimental work is required in order to validate the results obtained from the model.

A solver giving direct access to geometric and material properties allows this technique to be applied in an efficient manner by solving parametrically over ranges of different variables.

Effects due to complex conditions, such as fluid flow in the gap, can be modeled as modified material properties of the region we are concerned with.

Glue joints have proved to be a significant part of the thermal circuit and should not be neglected, although their small scale does require rectangular elements to produce an efficient mesh.

Complex regions of the driver, such as the voice coil, where the scale requires that a very large number of elements are required may be modeled as a composite material having the same bulk thermal properties. These techniques will prove vital for the production of 3D FEM models where the solution time will be much longer. While producing the 3D mesh is likely to prove somewhat onerous it will eliminate any need to spend time simplifying the geometry. The question of 2D versus 3D modeling is an important issue and will be the subject of future work by the author.

Further refinements that could be made would be to couple the thermal FEM model to an electric FEM model with coupled circuit & drive from voltage source. This will not only give the resistance rise as a result but will also correctly model the power dissipation in the voice coil.

Acknowledgments.

Many thanks to Dave Staton for his expert advice on thermal modeling, the support team at CEDRAT and Leon Lever for helping with both the experimental work and the preparation of the manuscript.

References

- [1] Clifford, A, Henricksen, "Heat Transfer Mechanisms in Loudspeakers; Analysis, Measurement and Design." Presented at the 80th Convention 1986 pre-print 2343.
- [2] Douglas, J, Button, "A Loudspeaker Motor Structure for Very High Power Handling and High Linear Excursion", Presented at the 83th Convention 1987 pre-print 2553.
- [3] JR Simonson, "Engineering Heat Transfer" 2nd Edition, MacMillan 1988
- [4] FLUX2D 7.60 User Manual, CEDRAT, Meyan France. 2002.
- [5] Dodd, Mark A, "The Transient Magnetic Behaviour of Loudspeaker Motors" Presented at the 111th Convention 2001.
- [6] Dave Staton. MotorCAD course "Thermal Analysis of Electric Motors" www.motor-design.com 2002.

